Progress In Electromagnetics Research, PIER 74, 407–419, 2007

BANDWIDTH WIDENING TECHNIQUES FOR DIRECTIVE ANTENNAS BASED ON PARTIALLY REFLECTING SURFACES

H. Boutayeb, T. A. Denidni, and M. Nedil

INRS-EMT, University of Quebec
800 rue de la Gauchetiere, Montreal Quebec H5A 1K6, Canada

Abstract—The directivity bandwidth of Fabry-Perot directive antennas is first evaluated theoretically. Then, different techniques are proposed to widen the directivity bandwidth of antennas using Partially Reflecting Surfaces. The bandwidths obtained with the proposed solutions are compared to the bandwidth of a classical Fabry-Perot directive antenna.

1. INTRODUCTION

High-gain and compact antennas with a single feed present an attractive solution for several wireless communication systems. Their single-feed system allows to increase the gain with low complexity compared to feeding networks used in conventional antenna arrays. In addition, the compactness represents an important advantage compared to parabolic antennas. To design low-profile high-gain antennas with a single feed, various methods have been proposed, such as the employment of Fabry-Perot type cavities [1–6], electromagnetic crystals or zero index metamaterials [7–12].

The inconvenient of high-gain antennas based on Fabry-Perot cavities, Electromagnetic Band Gap (EBG) materials, or metamaterials is their narrow directivity bandwidth. This can represent a drawback of these antennas compared to parabolic antennas, which have a large directivity bandwidth.

In this work, we propose different techniques to widen the bandwidth of these types of antennas. Three different configurations employing Partially Reflecting Surfaces (PRSs) composed of metallic wires are analyzed.

In Section 2, the directivity bandwidth of Fabry-Perot directive antennas is analyzed theoretically. Then, a Fabry-Perot cavity with

aperiodic PRSs is considered and presented in Section 3. A structure using two different PRSs is studied in Section 4. In Section 5, the two techniques are combined. The obtained directivity bandwidths of the different configurations are compared with that of a simple Fabry-Perot directive antenna. In all the structures presented in this paper, a dipole is used for the excitation.

2. EVALUATION OF THE DIRECTIVITY BANDWIDTH OF A FABRY-PEROT DIRECTIVE ANTENNA

It is well known that the bandwidth of a directive antenna based on a Fabry-Perot cavity decreases significantly when the desired gain is high. In this section, a relation between the minimum half-power beamwidth and the bandwidth is derived. The structure shown in Fig. 1 is considered. It is composed of a Fabry-Perot type cavity composed of two Partially Reflecting Surfaces (PRSs) made of metallic wires. An omni directional source is in the center of the cavity.

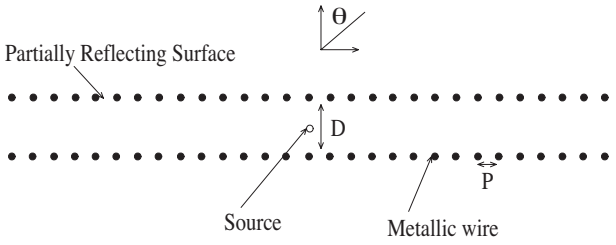

Figure 1. Principle of the Fabry-Perot directive antenna.

The frequency and angular response of the Fabry-Perot cavity to a plane wave excitation, which is in the center of the cavity, is called $|T|$, and it is obtained by summing all the transmitted rays [1]:

$$|T|^2 = \frac{1 - |r|^2}{1 + |r|^2 - 2|r| \cos(kD \cos(\theta) - \varphi_r)} \tag{1}$$

where k is the free space wave number and $r = |r| \exp(j\varphi_r)$ is the reflection coefficient of the partially reflecting surface constituted by the row of metallic wires.

For instance, we consider $|r| = 0.824$, $\varphi_r = 0.252\,\text{rad}$ and $D = 40\,\text{mm}$. In Fig. 2, $|T|$ is plotted versus frequency at $\theta = 0°$. The bandwidth of $|T|$ versus frequency at its half squared maximum amplitude is defined as $1/Q$, where Q is the quality factor of the cavity. Figure 3 shows $|T|$ versus angle at different frequencies. These

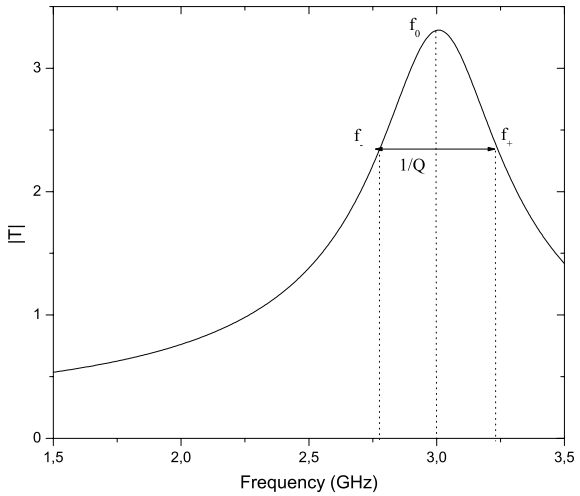

Figure 2. $|T|$ versus frequency, at $\theta = 0°$.

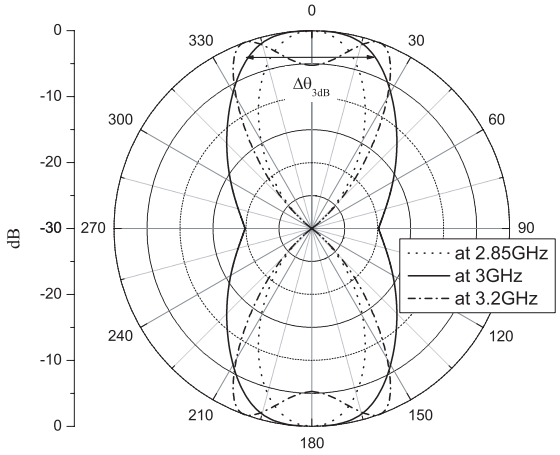

Figure 3. Normalized $|T|$ versus θ (logarithm scale) at different frequencies.

radiation patterns exhibit directive beams at the normal directions ($\theta = 0°$ and $\theta = 180°$) for frequencies lower than the resonant frequency f_0.

For frequencies greater than f_0, lobes appear on each side of the normal axis. $\Delta\theta_{3dB}$ is defined as the half-power beamwidth of the main beams at the normal directions (see Fig. 3).

In [1], it has been shown that the half-power beamwidth can be

expressed as following:

$$\Delta\theta_{3dB,f\leq f_0} \approx 2\sqrt{\frac{\sqrt{2x-1}-\sqrt{x-1}}{Q}} \tag{2}$$

$$\Delta\theta_{3dB,f_0\leq f\leq f_+} \approx 2\sqrt{\frac{\sqrt{x-1}+1}{Q}} \tag{3}$$

where $x = |T|^2_{max}/|T|^2$.

The minimum half-power beamwidth is obtained for $f < f_0$ (Eq. (2)) and for $x = 1.5$:

$$\Delta\theta_{3dB,min} \approx \sqrt{\frac{2\sqrt{2}}{Q}} \tag{4}$$

Note that Eq. (4) is a little different from the formula given in [1], where there is a minor error.

By using Eqs. (2) and (3), the half-power beamwidth $\Delta\theta_{3dB}$ is plotted in Fig. 4 as a function of the frequency, for the considered example.

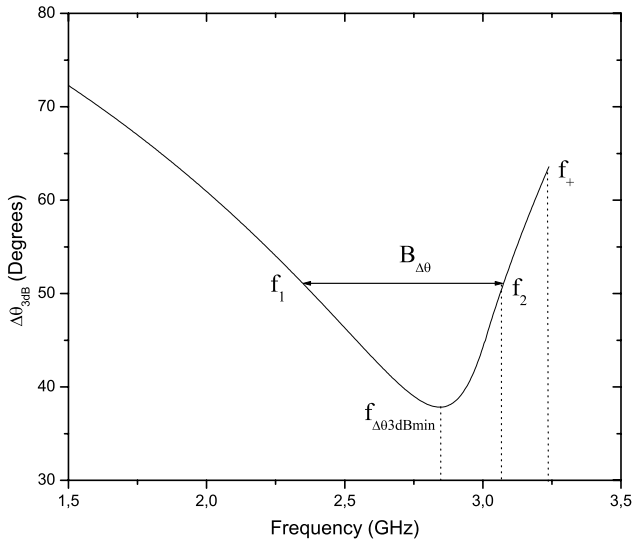

Figure 4. $\Delta\Theta_{3dB}$ versus frequency, computed by using Eqs. (2) and (3).

In Fig. 4, f_1 and f_2 are the frequencies for which $\Delta\theta_{3dB} = \sqrt{2}\Delta\theta_{3dB,min} \approx 2\sqrt{\frac{\sqrt{2}}{Q}}$. The coefficients x_1 and x_2, corresponding to f_1 and f_2, respectively, were calculated numerically from Eqs. (2) and (3): $x_1 \approx 10.985$, $x_2 \approx 1.175$.

Using the relation $\frac{1}{Q_x} \approx \sqrt{x-1}\frac{1}{Q}$ [1], we obtain:

$$2\frac{f_0 - f_1}{f_0} = \frac{1}{Q_{x1}} \approx \frac{\sqrt{9.895}}{Q} \tag{5}$$

and then

$$f_1 \approx f_0\left(1 - \frac{\sqrt{9.895}}{2Q}\right) \tag{6}$$

We have also

$$2\frac{f_2 - f_0}{f_0} = \frac{1}{Q_{x2}} \approx \frac{\sqrt{0.175}}{Q} \tag{7}$$

and then

$$f_2 \approx f_0\left(1 + \frac{\sqrt{0.175}}{2Q}\right) \tag{8}$$

Now, the bandwidth between f_1 and f_2 can be calculated as:

$$B_{\Delta\theta} = 2\frac{f_2 - f_1}{f_2 + f_1} \approx \frac{\sqrt{9.895} + \sqrt{0.175}}{4Q - \sqrt{9.895} + \sqrt{0.175}} \tag{9}$$

By using Eq. (4), the following relation is obtained

$$B_{\Delta\theta} \approx \frac{(\sqrt{9.895} + \sqrt{0.175})(\Delta\theta_{3dB,min}/2)^2}{2\sqrt{2} - (\sqrt{9.895} - \sqrt{0.175})(\Delta\theta_{3dB,min}/2)^2} \tag{10}$$

$B_{\underline{\Delta}\theta}$ is the frequency band where the half-power beamwidth is less than $\sqrt{2}$ times the minimum half-power beamwidth.

By using Eq. (10), the bandwidth is plotted versus the minimum half-power beamwidth in Fig. 5. This curve characterizes the performance of Fabry-Perot directive antennas. It can be seen that the beamwidth decreases drastically when the minimum half-power beamwidth is small.

For instance, we consider that the wires are 56 cm length and 2 mm diameter, the number of wires in each row is 29, the cavity is $D = 40$ mm width, the period is $P = 20$ mm, and the dipole is 65 mm length and 2 mm diameter. The structure was simulated with a Finite Difference Time Domain (FDTD) code. The simulated half-power beamwidths in H- and E-planes, are plotted *vs.* frequency in

Fig. 6. From this figure, the bandwidths are 20% and 23.8%, in the H- and E-planes, respectively. These results agree with the results predicted by Eq. (10) and illustrated in Fig. 5.

It is important to design a directive antenna that presents the

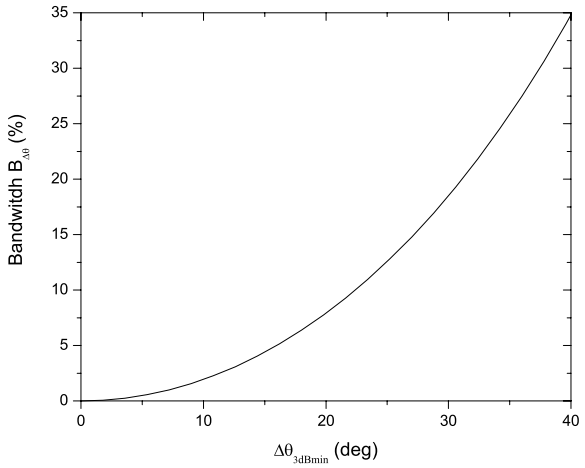

Figure 5. $B_{\Delta\Theta}$ versus $\Delta\Theta_{3dB,min}$, computed by using Eq. (10).

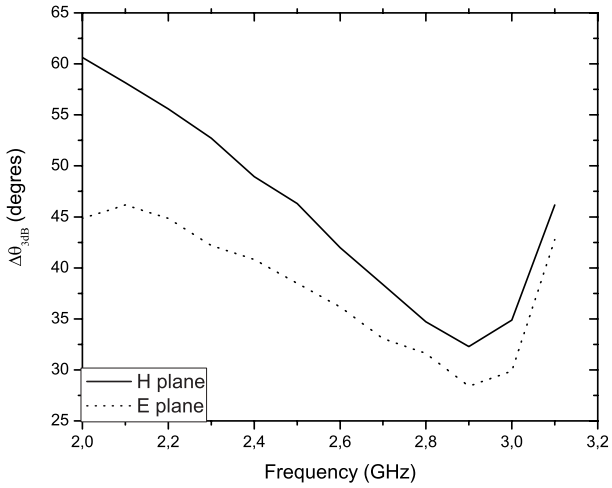

Figure 6. $\Delta\Theta_{3dB}$ versus frequency for a directive antenna using a dipole and two PRSs of metallic wires (FDTD).

same minimum beamwidth than the Fabry-Perot antenna but with a larger bandwidth. It is clear that antennas using electromagnetic crystals or zero index metamaterials [7–12] are not good candidates: they present the same performance than the Faby-Perot antenna in terms of relationship between directivity an bandwidth. In the next sections, we investigate two techniques to widen the bandwidth of a directive antenna based on Partially Reflecting Surfaces.

3. USING AN APERIODIC PARTIALLY REFLECTING SURFACE

A first method in order to increase the directivity bandwidth of the antenna consists on using a non-uniform PRS.

If one uses a PRS that presents a phase of the reflection coefficient increasing with the incidence angle, the bandwidth will increase. Indeed, the resonant frequency at the angle θ, can be written [1]:

$$f_{0,\theta} = \frac{\varphi_r(\theta)}{2\pi D \cos(\theta)} \tag{11}$$

where c is the speed of light and φ_r is the phase of the reflection coefficient r. From Eq. (11), if φ_r increases significantly with the angle θ, the resonant frequencies for angle higher than 0° will be shifted to higher frequencies, and the frequency f^+ (see Fig. 4) will be shifted to a higher frequency.

We propose to change the period of the PRS, as illustrated in Fig. 7, to obtain a coefficient φ_r increasing with incidence angle. The periods vary as followings: $P_1 = P_2 = 20\,\text{mm}$, $P_3 = P_4 = P_5 = P_6 = 17.5\,\text{mm}$, $P_7 = P_8 = P_9 = P_{10} = 15\,\text{mm}$, $P_{11} = P_{12} = P_{13} = P_{14} = 12.5\,\text{mm}$, and $P_{15} = P_{16} = P_{17} = P_{18} = 10\,\text{mm}$.

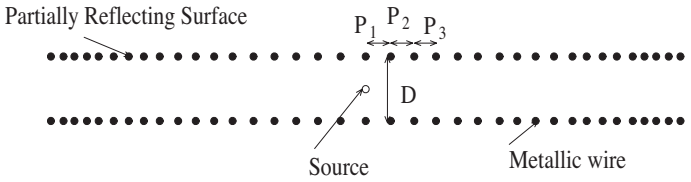

Figure 7. Directive antenna using an aperiodic PRS.

Note that the dimensions of the antenna (length, larger and dipole dimensions) are the same than previously.

In Figs. 8 and 9, the computed half-power beamwidths are plotted in the H- and E-planes, respectively, for the structure with aperiodic

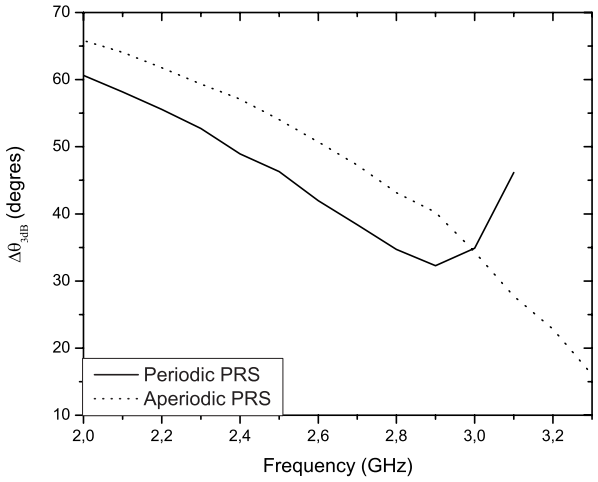

Figure 8. $\Delta\Theta_{3dB}$ versus frequency in the H-plane (FDTD).

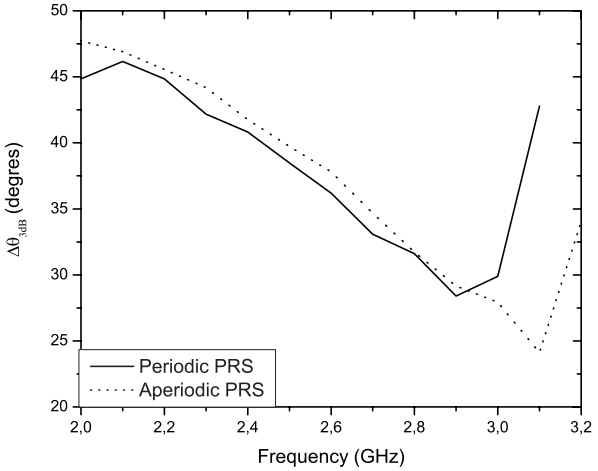

Figure 9. $\Delta\Theta_{3dB}$ versus frequency in the E-plane (FDTD).

PRSs and for the structure with periodic PRS. From these figures, it can be observed that the aperiodic PRS allows to decrease the half-power beamwidth after the resonant frequency ($f_0 = 3\,\mathrm{GHz}$). In the E-plane (Fig. 9), a widening of the bandwidth is also observed.

4. USING TWO DIFFERENT PARTIALLY REFLECTING SURFACES

Another method for increasing the directivity bandwidth consists on using two different PRSs.

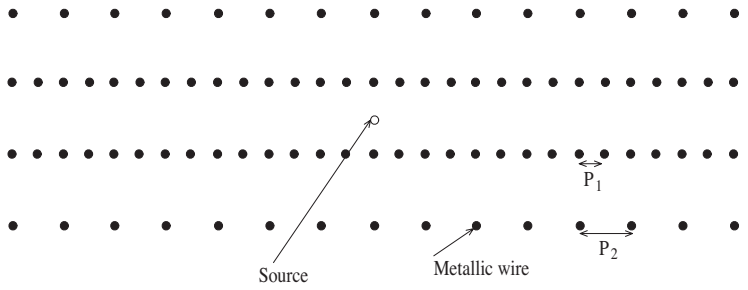

Figure 10. Directive antenna using two different PRSs.

Using multiple cavities allows to modify the response of the structure (*i.e.*, T), and then the curve of the half-power beamwidth. If the phase of reflection coefficient of the structure formed by the combination of the two PRSs increases with frequency, then it is possible to obtain a resonance of the Fabry-Perot cavity in a larger bandwidth. We consider the configuration shown in Fig. 10. The PRSs are spaced by the distance $D = 35\,\text{mm}$, and the two periods are $P_1 = 20\,\text{mm}$ and $P_2 = 40\,\text{mm}$. Figures 11 and 12 present the simulated half-power beamwidth of the antenna in the H- and E-planes, respectively. From these results, the bandwidths are 27%, in both H-plane and E-plane. The structure with two different PRSs and the structure with one PRS have the same minimum half-power beamwidth, but the structure with two different PRSs has a larger bandwidth. From this, the structure using two different PRSs has a better performance.

5. COMBINATION OF THE TWO TECHNIQUES

To increase further the bandwidth of the antenna, a structure combining the two previous techniques is considered. The structure is shown in Fig. 13.

The larger and length of the antenna are the same than in previous sections ($56 \times 56\,\text{cm}^2$) and $D = 35\,\text{mm}$. Figs. 14 and 15 present the half-power beamwidth in the H- and E-planes. From these curves, it can be concluded that the antenna offers bandwidths of 32% and 34%,

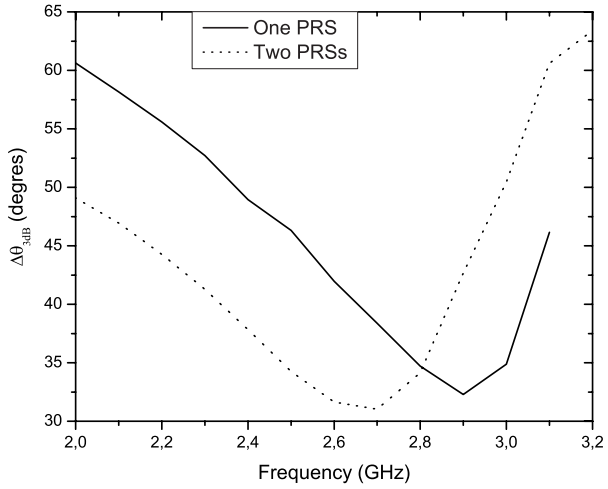

Figure 11. $\Delta\Theta_{3dB}$ versus frequency in the H-plane (FDTD).

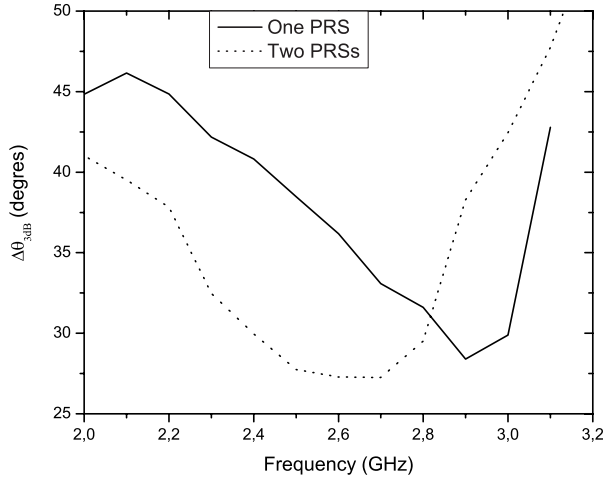

Figure 12. $\Delta\Theta_{3dB}$ versus frequency in the E-plane (FDTD).

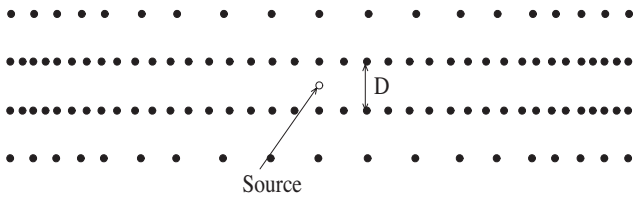

Figure 13. Directive antenna using two aperiodic PRSs.

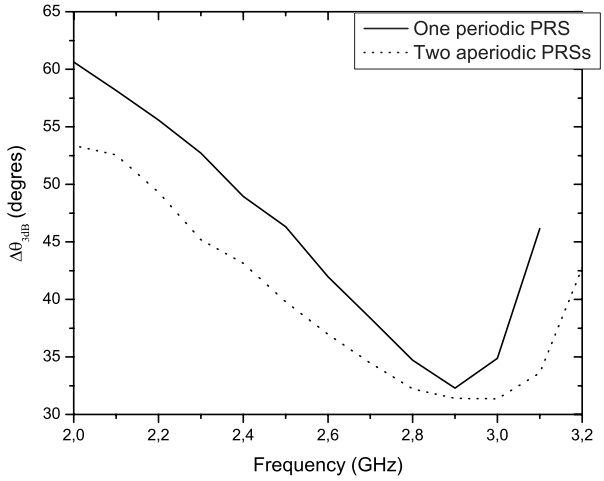

Figure 14. $\Delta\Theta_{3dB}$ versus frequency in the H-plane (FDTD).

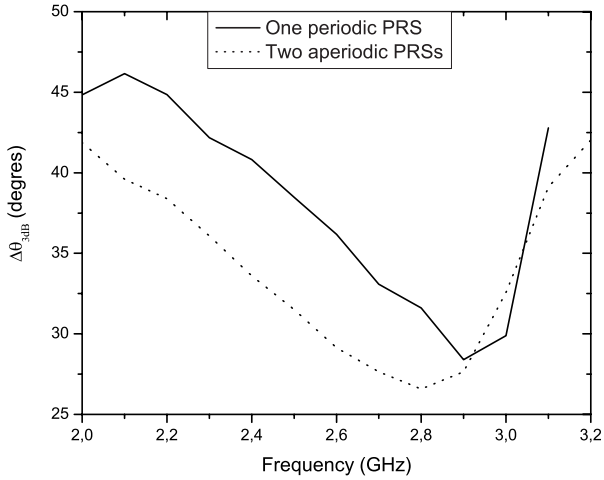

Figure 15. $\Delta\Theta_{3dB}$ versus frequency in the E-plane (FDTD).

in the H-plane and E-plane, respectively, which represent bandwidths enhancements of 60% and 43% compared to the bandwidths obtained using the classical Fabry-Perot cavity structure.

6. CONCLUSION

A new analytical expression for the directivity bandwidth of Fabry-Perot directive antennas using Partially Reflecting Surfaces has been presented. To widen the bandwidth of these antennas, two techniques have been proposed. The first one consists on varying the distance between elements in the Partially Reflecting Surface, while the second technique uses different PRSs. A third configuration combining the two techniques has also been analyzed to increase further the bandwidth. Numerical results obtained with a full wave method have been presented, showing the usefulness of the proposed approach.

ACKNOWLEDGMENT

The authors gratefully acknowledge the support of this research from National Science Engineering Research Council of Canada (NSERC).

REFERENCES

1. Boutayeb, H., K. Mahdjoubi, A. C. Tarot, and T. A. Denidni, "Directivity of an antenna embedded inside a Fabry-Perot cavity: theory and design," *Micro. Opt. Tech. Lett.*, Vol. 48, 12–17, 2006.
2. Gu, Y. Y., W. X. Zhang, and Z. C. Ge, "Two improved Fabry-Perot resonator printed antennas using EBG substrate and AMC substrate," *Journal of Electromagnetic Waves and Applications*, Vol. 21, 719–728, 2007.
3. Pirhadi, A. and M. Hakkak, "An analytical investigation of the radiation characteristics of infinitesimal dipole antenna embedded in partially reflective surfaces to obtain high directivity," *Progress In Electromagnetics Research*, PIER 65, 137–155, 2006.
4. Guerin, N., S. Enoch, G. Tayeb, P. Sabouroux, P. Vincent, and H. Legay, "A metallic Fabry-Perot directive antenna," *IEEE Trans. Antennas Propag.*, Vol. 54, 220–224, Jan. 2006.
5. Feresidis, A. P., G. Goussetis, S. Wang, and J. C. Vardaxoglou, "Artificial magnetic conductor surfaces and their application to low-profile high-gain planar antennas," *IEEE Trans. Antennas Propag.*, Vol. 53, 209–215, Jan. 2005.
6. Pirhadi, A., F. Keshmiri, M. Hakkak, and M. Tayarani, "Analysis and design of dual band high directive ebg resonator antenna using square loop fss as superstrate layer," *Progress In Electromagnetics Research*, PIER 70, 1–20, 2007.

7. Li, B., B. Wu, and C.-H. Liang, "High gain circular waveguide array antenna using Electromagnetic Band Gap Structures," *Journal of Electromagnetic Waves and Applications*, Vol. 20, 955–966, 2006.
8. Cheype, C., C. Serier, M. Thevenot, T. Monediere, A. Reineix, and B. Jecko, "An electromagnetic bandgap resonator antenna," *IEEE Trans. on Antennas Prop.*, Vol. 50, 1285–1290, Sept. 2002.
9. Enoch, S., G. Tayeb, P. Sabouroux, N. Guerin, and P. Vincent, "A metamaterial for directive emission," *Phys. Rev. Lett.*, Vol. 89, No. 21, 213902-1-213902-4, Nov. 2002.
10. Enoch, S., G. Tayeb, and D. Maystre, "Dispersion diagrams of bloch modes applied to the design of directive sources," *Progress In Electromagnetics Research*, PIER 41, 61–81, 2003.
11. Wu, B.-I., W. Wang, J. Pacheco, X. Chen, T. M. Grzegorczyk, and J. A. Kong, "A study of using metamaterials as antenna substrate to enhance gain," *Progress In Electromagnetics Research*, PIER 51, 295–328, 2005.
12. Li, B., B. Wu, and C.-H. Liang, "Study on high gain circular waveguide array antenna with metamaterial structure," *Progress In Electromagnetics Research*, PIER 60, 207–219, 2006.
13. Boutayeb, H. and T. A. Denidni, "Analysis and design of a high-gain antenna based on metallic crystals," *Journal of Electromagnetic Wave and Application*, Vol. 20, 599–614, 2006.